Electrolytes Affect the Life-Time of Lithium Batteries

The valence behavior of lithium battery materials can be resolved by soft X-ray absorption spectroscopy.

The 2019 Nobel Prize in Chemistry was awarded to John B. Goodenough, M. Stanley Whittingham, and Akira Yoshino for their contributions to the development of lithium-ion batteries. Compared with other rechargeable batteries, such as nickel-metal hydride batteries, lithium-ion batteries have higher cycle times and energy density, making them more suitable for mobile communication and portable electronic devices. The first commercial lithium-ion battery structure consisted of a petroleum coke or graphite anode, cobalt oxide as the cathode, and a lithium-ion electrolyte. Although lithium-ion batteries have been widely used, scientists are constantly in search of safer, more efficient, and longer-lasting battery materials. This report summarizes the results from two lithium battery studies[1,2] conducted by the team of Guanglei Cui in Chinese Academy of Sciences, China.

The electrolyte in lithium-ion batteries not only transfers lithium ions but also regulates the electrode interface and largely determines the life and stability of the battery. Although many currently used electrolytes have relatively balanced properties, they can still easily trigger oxidation–reduction reactions at the electrode interface under high-temperature and high-humidity environments, ultimately affecting battery life and causing safety issues. Currently, there are still restrictions on the transportation of lithium batteries. Researchers compared the electrolyte properties of newly synthesized lithium difluoro(1,2-dihydroxyethane-1,1,2,2-tetracarbonitrile) borate (LiDFTCB) with commonly used lithium difluoro(oxalato) borate (LiDFOB).

To study the interfacial reaction mechanism, the research team conducted X-ray absorption spectroscopy (XAS) measurements at **TLS 11A1**. The world's first Dragon beamline designed by Dr. Chien-Te Chen, who was then based at the Bell Laboratories, was transferred from NSLS to **TLS 11A1** and re-constructed in 1998. It features separate horizontal and vertical focusing mirrors that eliminate astigmatic coma aberration and an exit slit movable to the focal point of each wavelength that eliminates defocus aberration. Combined with a suitable focusing ratio and minimum number of optical elements, a high flux and high resolution beamline with a simple scanning mechanism is created. The **TLS 11A1** Dragon beamline has been operating since 1999 and is one of the longest-running beamlines in the world. The XAS endstation of **TLS 11A1** can measure both total electron yield (TEY) and total fluorescence yield (TFY) signals. TEY is measured directly from the photocurrent of the sample using a pico current meter. The signal mainly comes from the surface 2–4 nm and is therefore suitable for studying the electrode interface. The TFY is measured using a multi-channel plate. This allows for a better depth detection profile and can be regarded as the bulk properties of the material.

For the Co L-edge XAS spectra, shown in **Fig. 1 (a)**, although the cycled $LiCoO_2$ cathodes maintain the predominant Co^{3+} state, the higher energy shifts and an increase in the intensity of peaks at 779.5 eV indicate the appearance of Co^{4+} species after cycling. In the O K-edge XAS spectra, the pre-edge peaks below 533 eV shift to a lower energy with an increase in the Co valence state. Compared to the pristine $LiCoO_2$, the cycled $LiCoO_2$ cathodes clearly exhibit two new pre-edge peaks at 528 and 529 eV, which are characteristic Co^{4+} related peaks. This further confirms the existence of Co^{4+} species after cycling (**Fig. 2(b)**, see next page). The pre-edge peaks in the O K-edge XAS spectra (**Fig. 1(b)**) of cycled $LiCoO_2$ taken in the TFY mode display much higher spectral weight than those taken in the TEY mode. This indicates a higher Co^{4+} content in the bulk structure after cycling in LiDFOB-PC than that cycled in LiDFTCB-PC. The XAS results confirm the negative effect of the interface reaction between LiDFOB and $LiCoO_2$ on the reversible $Co^{3+/4+}$ redox reaction, which is also detrimental to the bulk structure reversibility. Based on these spectra, it is inferred that lithium ions accumulate at the electrolyte/electrode interface after multiple charge cycles, causing the valence of Co to increase.

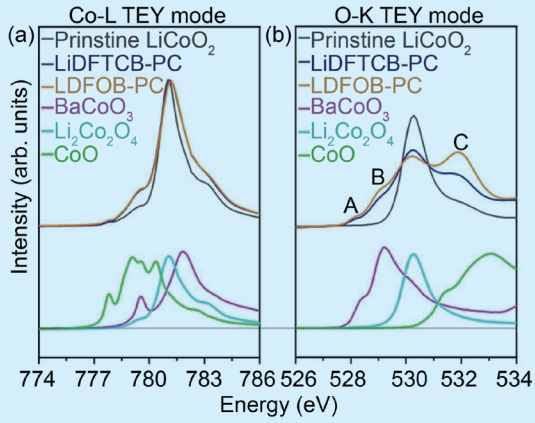

Fig. 1: The Co L-edge (a) and O K-edge (b) XAS TEY spectra of the pristine and cycled $LiCoO_2$ cathodes, together with those of CoO, $Li_2Co_2O_4$, and $BaCoO_3$ as the references. [Reproduced from Ref. 1]

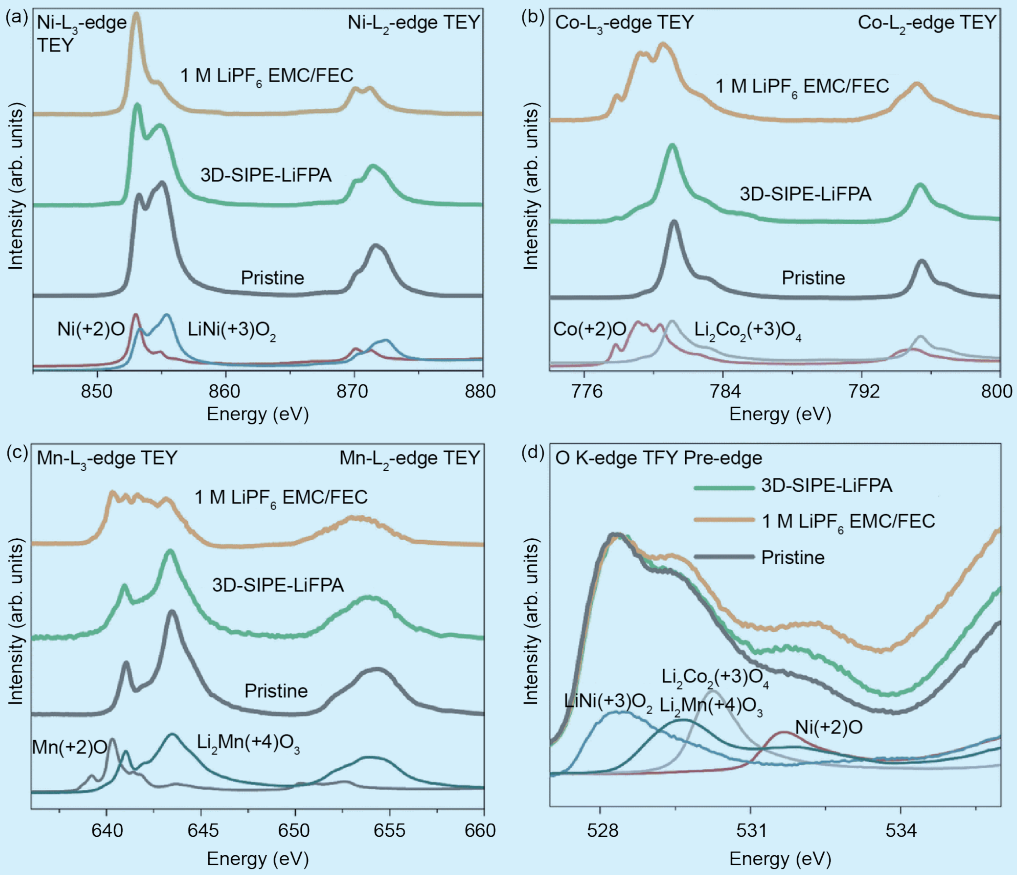

Fig. 2: (a–c) Ni, Co, Mn $L_{3,2}$-edge XAS spectra in the TEY mode and (d) O K-edge XAS spectra in the TFY mode of the measured NCM811 cathodes: pristine (black line), cycled in 3D-SIPE-LiFPA (green line), and cycled in 1 M $LiPF_6$ EMC/FEC electrolyte (yellow line). The measured NCM811 cathodes were harvested from NCM811/Li LMBs (50 μm, 3.7 mA h cm^{-2}, 2.8–4.3 V) after 50 cycles. [Reproduced from Ref. 1]

Another studies by the same team also used XAS to analyze electrode materials. Currently, commercial lithium-ion batteries mostly use graphite as the anode material. Lithium ions are embedded in the graphite after passing through the electrolyte. The development of lithium metal batteries actually preceded that of lithium ion batteries. However, due to the high activity of lithium metal, lithium metal often passes through the electrolyte and reaches the cathode, causing a short circuit. Because the structure of lithium metal batteries only requires a very thin lithium component as an anode, they display improved overall energy density and have been the subject of many studies. The research team synthesized a novel electrolyte, 3D-SIPE-LiFPA, to use in lithium metal batteries. This electrolyte is combined with a NCM811($LiNi_{0.8}Co_{0.1}Mn_{0.1}O_2$) cathode to make a full lithium metal battery, and the control group $LiPF_6$ electrolyte was used for comparison. Lithium metal battery research often focuses on improving cycle life; however, the thermal stability of the battery is often neglected. The research team conducted several thermal tests on different electrolytes. A significant enhancement of the safety characteristics of the soft pack battery was achieved using 3D-SIPE-LiFPA as an electrolyte, since it reduces the heat released by the lithium anode. When cycled in 3D-SIPE-LiFPA, the decrease in the oxidation state from Ni^{3+} to Ni^{2+} was significantly suppressed. Similarly, the transition of Co^{3+} to Co^{2+}, as well as the transition of Mn^{4+} to Mn^{3+} and Mn^{2+} (**Figs. 2(a)–2(c)**) were also greatly inhibited when using 3D-SIPE-LiFPA. The O K-edge XAS spectra (**Fig. 2(d)**) in the bulk structure-affected TFY showed a lower Ni^{2+} content when using 3D-SIPE-LiFPA, in line with the Ni L-edge XAS result. XAS, along with other analyses, provide a clearer picture of the interfacial reaction. The interfacial layer of the F3D-SIPE-LiFPA-derived cathode prevents the reduction of the Co ion valence state and inhibits the dissolution of the transition metal and destruction of the crystal structure.

XAS is sensitive to the element valence, bonding, and material structure. With the combination of TEY and TFY, it provides considerable validation of the reaction mechanisms at the lithium battery material interface. (Reported by Fan-Hsiu Chang)

This report features the work of Guanglei Cui and his collaborators published in Angew. Chem.Int. Ed. ***62****, e2023026 (2023) and Energy Enivron. Sci.* ***16****, 2591 (2023).*

TLS 11A1 (Dragon) MCD, XAS

- XAS, XMCD
- Materials Science, Batteries

References

1. X. Min, C. Han, S. Zhang, J. Ma, N. Hu, J. Li, X. Du, B. Xie, H.-J Lin, C-Y Kuo, C-T Chen, Z. Hu, L. Qiao, Z. Cui, G. Xu, G. Cui, Angew. Chem. Int. Ed. **62**, e2023026 (2023).
2. S. Zhang, F. Sun, X. Du, X. Zhang, L. Huang, J. Ma, S. Dong, A. Hilger, I. Manke, L. Li, B. Xie, J. Li, Z Hu, A. C. Komarek, H.-J. Lin, C.-Y. Kuo, C.-T Chen, P. Han, G. Xu, Z. Cui, G. Cui, Energy Enivron. Sci. **16**, 2591 (2023).

Novel Energy Materials Research With X-ray Photoelectron Spectroscopy

*X-ray photoelectron spectroscopy at **TLS 24A1** helps researchers identify the chemical composition at the surface/interface of new energy materials.*

TLS 24A1 provides a wide-range soft X-ray beamline with photon energies ranging from 15 to 1600 eV. X-ray photoelectron spectroscopy (XPS) is the primary application of this beamline. **TLS 24A1** is equipped with two endstations: an ultra-high vacuum XPS for standard surface analysis and a near-ambient-pressure XPS (APXPS) to characterize surfaces in sub-Torr pressure ranges. The versatility of XPS has attracted multidisciplinary research groups to conduct experiments at **TLS 24A1**. Here, we highlight five papers which reported the development of novel materials with an emphasis on the role of XPS.

The global energy crisis has resulted in recent research efforts devoted to solid-state batteries. The interface at the electrolyte–electrode boundary is a crucial factor that determines battery performance. The following three examples of Bing Joe Hwang, Wei-Nien Su (both from National Taiwan University of Science and Technology) and their collaborators demonstrate the role of XPS in elucidating the chemical composition around the electrode–electrolyte interface. The first example is the development of anode-free lithium metal batteries containing a lithium argyrodite solid-state electrolyte.[1] To enhance the contact between the solid-state electrolyte and the Cu@Ag of the outer circuit, a deformable sulfide composite solid electrolyte (SCSE-4) was fabricated by incorporating the common lithium argyrodite (LPSC) into a eutectic solution with a polyvinylidene fluoride binder and LiF salt additive. XPS shows that the thiophosphate group in the SCSE-4 composite retained its identity in the eutectic mixture, indicating that the void volume in the sulfide composite solid electrolyte is negligible. Consequently, the contact between the solid-state electrolyte and the outer circuit is enhanced. In the second example, the research team synthesized a novel, highly fluorinated electrolyte to mitigate the capacity fading of high-voltage lithium-ion batteries.[2] XPS confirms that the fluorinated electrolyte effectively stabilizes both S-C(PAN) anode and LNMO cathode surfaces in the fuel cell. Lastly, the research team developed a new type of solid-state electrolyte made of iodized-oxychloride argyrodite.[3] The sacrificial iodine in the electrolyte effectively suppresses dendrite formation. XPS confirmed the synergistic contribution of sacrificial iodine and oxygen-doped sulfide solid electrolytes in forming a stable interface.

Aside from solid-state batteries, Hwang and Su's team attempted to enhance the electrochemical performance of a Zn aqueous battery by improving the uniformity of the Zn deposit.[4] Adding a low concentration of glutamic additive modifies the electrode surface's hydrogen-bonding network. Consequently, a uniform layer of Zn deposit is established on the electrode. In this work, XPS confirmed the binding of the glutamic additive on the surface.

Dye-sensitized solar cells have been intensely researched to enhance the harvesting of solar energy. Eric Wei-Guang Diau (National Yang Ming Chiao Tung University) and his collaborators developed X-shaped quinoxaline-based organic dyes, which serve as a p-type self-assembly mono (SAM) layer for tin perovskite solar cells.[5] The device performance reached 8.3% when the dye TQxD was used to construct the SAM layer, a record-high efficiency for SAM-based tin perovskite solar cells. In this work, the functional groups identified in the C 1s XPS confirm the chemical bonding between the SAM layer and the ITO substrate. (Reported by Bo-Hong Liu)

*This report features the work of Bing Joe Hwang, Wei-Nien Su, and their collaborators published in J. Power Sources **556**, 232462 (2023); J. Power Sources **558**, 232567 (2023); Nano Energy **112**, 108471 (2023); and ACS Appl. Mater. Interfaces **15**, 7949 (2023); as well as the work of Eric Wei-Guang Diau and his collaborators published in Adv. Funct. Mater. **33**, 2213939 (2023).*